

SURFACE WAVE SCATTERING FROM ELLIPTICAL CRACKS FOR FAILURE PREDICTION

B. R. Tittmann*, O. Buck and L. Ahlberg
Rockwell International Science Center
Thousand Oaks, California 91360 USA

M. De Billy, F. Cohen-Tenoudji, A. Jungman, and G. Quentin
Groupe de Physique des Solide de L'Ecole Normale Supérieure**
Universite Paris VII, Tour 23, 2 Place Jussieu
75221 Paris Cedex 05, France

ABSTRACT

The scattered radiation patterns of surface cracks irradiated by acoustic surface waves are interpreted to provide estimates of crack length and aspect ratio, geometric crack parameters needed to enable failure prediction. The technique is demonstrated for circular and elliptical cracks as small as 100 μm in depth with an accuracy of about 10%. The key features are the positions and spacing of peaks and nulls in angular and frequency dependence of scattered surface intensity. A simple model based on optical diffraction theory is demonstrated on cracks in commercial hot-pressed silicon nitride studies at 100MHz and on spark eroded slots in commercial aluminum studies at 2-10 MHz. The results are used to calculate the stress intensity factors and to describe the direction of crack propagation for a variety of real and simulated cracks. Implications of the technique with respect to crack closure and effects of stress and time are also discussed.

INTRODUCTION

Surface cracks are playing an ever increasingly important role in the fracture of structural materials and are now being given concentrated attention from the point of view of characterization towards more effective failure prediction. In a recent paper Doyle and Scala¹ presented a review of both bulk and surface wave ultrasonic methods of the measurement of the depth of (part-through) cracks. They give a rather extensive survey of the literature and considered the research which relates to techniques for measuring crack depth by studying the scattered pulse amplitude, by using time-of-flight methods, or by carrying out ultrasonic spectroscopic analysis. On the basis of the techniques developed up to the time of their survey, they suggested that measurements of the transit time of bulk waves appears most likely to provide simple and reliable depth measurements in the near future.

On the other hand, since this review was written there have been several reports on new techniques and approaches using surface waves which show considerable promise. Khuri-Yakub and Kino² have developed a new technique for exciting high-frequency (100 MHz range) surface and shear acoustic waves on non-piezoelectric materials. Fraser, Khuri-Yakub and Kino³ have produced a design for an efficient broad-band wedge transducer. Resch et al.⁴ have carried out measurements with a surface wave probe and predicted fracture stresses in good agreement with those measured. The calculations of the fracture stress were based in part on theoretical developments by Kino.⁵ Domarkas et al.⁶ have observed structure in the frequency dependence of the acoustic surface reflection coefficient

associated with a rectangular slot which they have interpreted in terms of resonances across the length and depth of the slot. Ayter, Auld and Tan⁷ have developed two theoretical approaches based on real reciprocity relations for the scattering of Rayleigh surface waves by part-through cracks. In a short letter we⁸ have reported experimental data and a simple model on the estimation of the size of small surface cracks.

In this paper we present the details of our work both for crack length and crack depth determination and cast these results into the context of the fracture mechanics of part-through cracks to delineate the stress intensity range (for a given stress application) and determine the remaining fatigue life of structural materials. The considerations include, specifically, the differences between cracks in ductile and brittle materials, the degree of crack closure, the crack orientation, and the specimen geometry. These factors are shown to play an important role in selecting those types of scattering measurements most directly useful for failure prediction.

CRACK PARAMETERS FOR FAILURE PREDICTION

Since failure prediction is the ultimate objective of the quantitative NDE (nondestructive evaluation) studies reported here, our approach has been to delineate the important fracture mechanics parameters and ask what ultrasonic measurements must be made, and how they must be interpreted to obtain these parameters as directly and accurately as is needed for failure prediction.

Table I presents values for parameters which are important in defining the approach to the study of cracks in technologically important materials. It lists some key alloys and ceramics ordered according to their ductility (percent elongation) and shows the importance of considering both the case of fatigue cycling to failure and brittle fracture. In columns three and four of Table I, respectively, are listed approximate values of

*Part of the work by B. R. Tittmann was carried out during his stay at Universite Paris VII as "professeur associe".

**Laboratoire associe au C.N.R.S.

TABLE I
ORDER OF MAGNITUDE ESTIMATES OF CRITICAL FLAW
SIZES IN METAL AND CERAMIC SYSTEMS,
ORDERED ACCORDING TO DUCTILITY

MATERIAL	% ELONG.	CRIT. FLAW SIZE (MM)	f_c
2024-T351 ALUMINUM	20	25.0	20 kHz
9H1-4Co-20C STEEL	19	18.0	25 kHz
9AL-1Mo-1V (B) TITANIUM	17	14.5	35 kHz
2014-T651 ALUMINUM	13	4.5	100 kHz
6AL-4V TITANIUM	13	-2.5	200 kHz
A340 STEEL	13	1.5	300 kHz
D6AC STEEL	10-13	1.0	500 kHz
HOT PRESSED SI-NITRIDE	~ 0	0.05	30 MHz
SINTERED SI-NITRIDE	~ 0	0.02	80 MHz
SILICA GLASS	~ 0	0.003	150 MHz
SODA LIME GLASS	~ 0	0.001	500 MHz

$$\sigma_{MAX} \sim 0.5 \sigma_{YIELD}$$

critical flaw sizes a_c for these materials based on an assumed stress of one-tenth of the yield stress and the critical ultrasonic frequencies f_c corresponding to the criterion $ka_c = 1$, where $k_c = 2\pi f_c/v$ is the ultrasonic wave vector (v is the ultrasonic wave velocity). Very qualitatively speaking the regime of frequencies below f_c is called the Rayleigh regime and long-wavelength techniques such as already described by Resch et al.⁴ are appropriate. Considering the low values of f_c shown for some of the more ductile alloys, such factors as specimen size and Rayleigh wave generation techniques are seen to be important limitations on the general usefulness of the Rayleigh regime.

Driven by these considerations this paper attempts to address the short wavelength regime, i.e., $ka_c \geq 1$, emphasizing cracks in ductile materials but demonstrating the applicability of the ultrasonic techniques to cracks in ceramics, where the critical crack sizes are small and therefore the wavelength must be very short. To demonstrate the somewhat specialized nature of the approach that must be taken for ductile materials, Fig. 1 displays a typical example of part-through

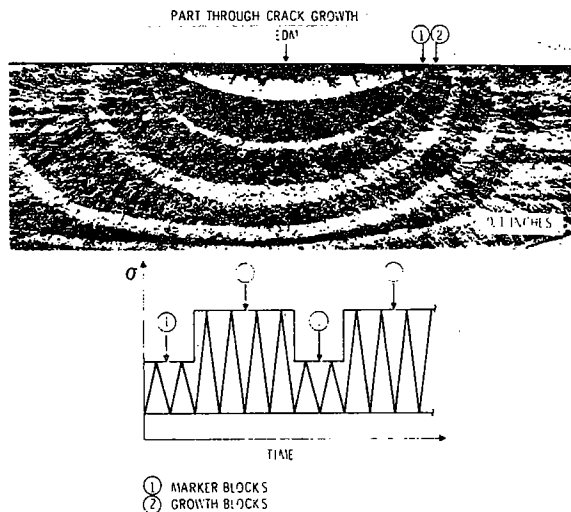


Fig. 1. Photo of crack surface for metal plate fatigue-cycled to failure.

growth of an EDM notched sample⁹ where the progress of crack propagation during cyclic fatigue is depicted in terms of marker and growth blocks (light and dark shaded regions), respectively, which correspond to growth under low and high applied stress. Since the crack growth takes place over a relatively long time it is important to speak in terms of a stress intensity range and a remaining life in terms of the number of cycles for failure. After Irwin¹⁰ the stress intensity range (in mode I) ΔK_I is

$$\Delta K_I = C \Delta \sigma \sqrt{a/Q} \quad (1)$$

where $C = 1.95$

$$Q = \Phi^2 - 0.212 \left(\frac{\sigma_{max}}{\sigma_{yield}} \right)^2$$

$$\Phi = \int_0^{\pi/2} [\sin^2 \psi + (a/c)^2 \cos^2 \psi]^{1/2} d\psi$$

and where $\Delta \sigma$ is the stress range, a is the crack depth, $2c$ is the crack length, σ_{yield} is the yield stress, σ_{max} is the maximum applied stress and ψ is the angle in the crack plane with respect to the crack length. The symbols are identified in Fig. 2a. For a given applied stress the stress intensity range ΔK_I may be calculated from a knowledge of the metallurgy of the part (i.e., σ_{yield}), the crack depth a and the depth-to-length ratio.

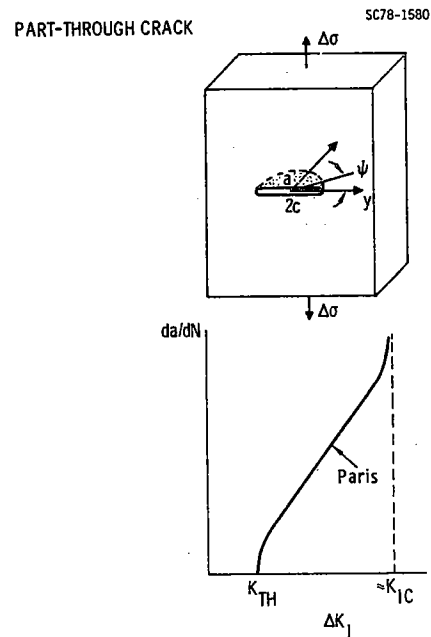


Fig. 2. (a) Geometry of part-through crack (b) Schematic graph of functional dependence of crack growth rate on stress intensity range ΔK_I .

Assuming the crack is in the Paris regime of validity, the crack-depth-increase-per-unit fatigue cycle da/dN is¹¹

$$da/dN = A(\Delta K_I)^m \quad (2)$$

where A and m are material constants. The remaining life or number of cycles to failure is then

$$\Delta N = \frac{2}{(m-2)A(CQ^{1/2}\Delta\sigma)^m} \left\{ \frac{1}{a^{(m-2)/2}} - \left(\frac{CQ^{-1/2}\sigma_{max}}{K_{1c}} \right)^{m-2} \right\} \quad (3)$$

Failure is imminent, i.e., $N = 0$, when

$$a_c = \left(\frac{K_{1c}}{CQ^{-1/2}\sigma_{max}} \right)^2 \quad (4)$$

A typical curve of da/dN as a function of ΔK_I is shown schematically in Fig. 2b. Equation (4) was used to estimate the critical flaw sizes of Table I.

In summary, aside from the metallurgical properties of the material, the important fracture mechanics parameters which NDE must give are the crack depth and length.

EXPERIMENTAL APPROACH

The approach used in these measurements embraces both the techniques of Rayleigh generation/detection and spectroscopic analysis. These techniques are in general not new, since surface waves have been used for quite some time as a basis of measurement of crack depth. For example, Reinhardt and Dally¹² noted that the variation of the surface wave transmission and reflection coefficients with crack depth might provide results for cracks less than half a wavelength deep. Buck, Frandsen, and Marcus¹³ have used surface waves to monitor crack growth and crack closure. Silk¹⁴ has made crack depth measurements by detecting S-waves produced by mode conversion of R-waves at the crack tip. Cook¹⁵, Huggell, Morgan and Lumb,¹⁶ Hall¹⁷ and Lidington and Silk¹⁸ have used surface timing methods for crack depth measurement. Ultrasonic spectroscopy originally applied primarily to bulk defects as discussed by Gericke¹⁹ and Brown²⁰ has also now been applied to surface flaws with Rayleigh waves. Morgan²¹ used the time reconstitution method and crystal method to not only detect the crack, but also map its morphology.

Our approach combines several of these methods in a new way by studying the scattered radiation pattern of surface waves from cracks in the time and frequency domain. In some of the experiments, commercial broad-band longitudinal wave transducers were used with water wedges to provide both the transmitter and receiver. The actual transducer configuration consisted of a small metal box which was filled with water and into which was mounted a Parametrics M-series transducer whose inclination angle to the specimen surface was adjusted to the Rayleigh angle. The metal box was glued to the

specimen surface with had low viscosity quick drying cement and in order to minimize the attenuation of the surface waves as they cross beneath the edge of the box, the edge was tapered into a knife-edge.

In other experiments at high frequencies (100 MHz) an interdigital transducer deposited on a $LiNbO_3$ delay line was used² on plates of commercial hot-pressed silicon nitride (NC 132) into which cracks were placed by the indentation technique which has been shown to give semi-circular crack shapes.²² In the narrow band experiments at 2.2 MHz wedge transducers were used on plates of commercial rolled Al into which semi-circular slots had been cut by the spark erosion technique. In other broad-band experiments the transducers were again commercial broadband transducers (2-9 MHz at 3 dB) inclined to the sample surface with both transducer and specimen immersed in water at the critical Rayleigh angle. The samples were plates of Duraluminum into which slots had been cut by indentation with a flat, semi-circular tip of a hard tool. In each of the experiments the angular dependence data were obtained by either rotating the sample or the transducer about an axis through the center of the crack. The precision of determining the angle is estimated at ± 0.5 degrees.

Figure 3 shows a photograph of the apparatus of one of the experiments and depicts the goniometer that was used with circular plates and the water-wedge transducers (in the form of boxes) discussed above. Also shown are the associated electronics such as a Parametrics Pulser-Receiver and a Tektronics sampling scope which was used to digitize the rf signals received and provide an interface with a Data General S/200 Eclipse computer. This minicomputer was used to obtain the Fourier transform of the signal, which was typically divided by the transducer transfer functions and to so calculate, and display the normalized magnitude of the resulting Fourier transform. The transducer transfer function was obtained in a separate experiment in which the surface waves were back-scattered from an ideal scatterer, typically, a sharp edge of quasi-infinite extent.

RESULTS

Theoretical Model

A rigorous treatment of the scattering of acoustic surface waves from semi-circular surface cracks at arbitrary wavelength-to-crack radius ratio is not presently available. However, approximate theories^{23,24} in the long and short wavelength limits are currently being given much attention and preliminary comparisons between theory and experiment show high promise.

In particular Auld et al⁷ have formulated two theoretical approaches based on real reciprocity relations; one of them utilizes the volume integral form of the reciprocity relation, which gives the scattering coefficient as an integral product of unperturbed and perturbed fields and Bor's approximation is applied to evaluate the perturbed fields. The other approach utilizes the ultrasonic analog of the induction theorem in electromagnetics, in which the crack is represented

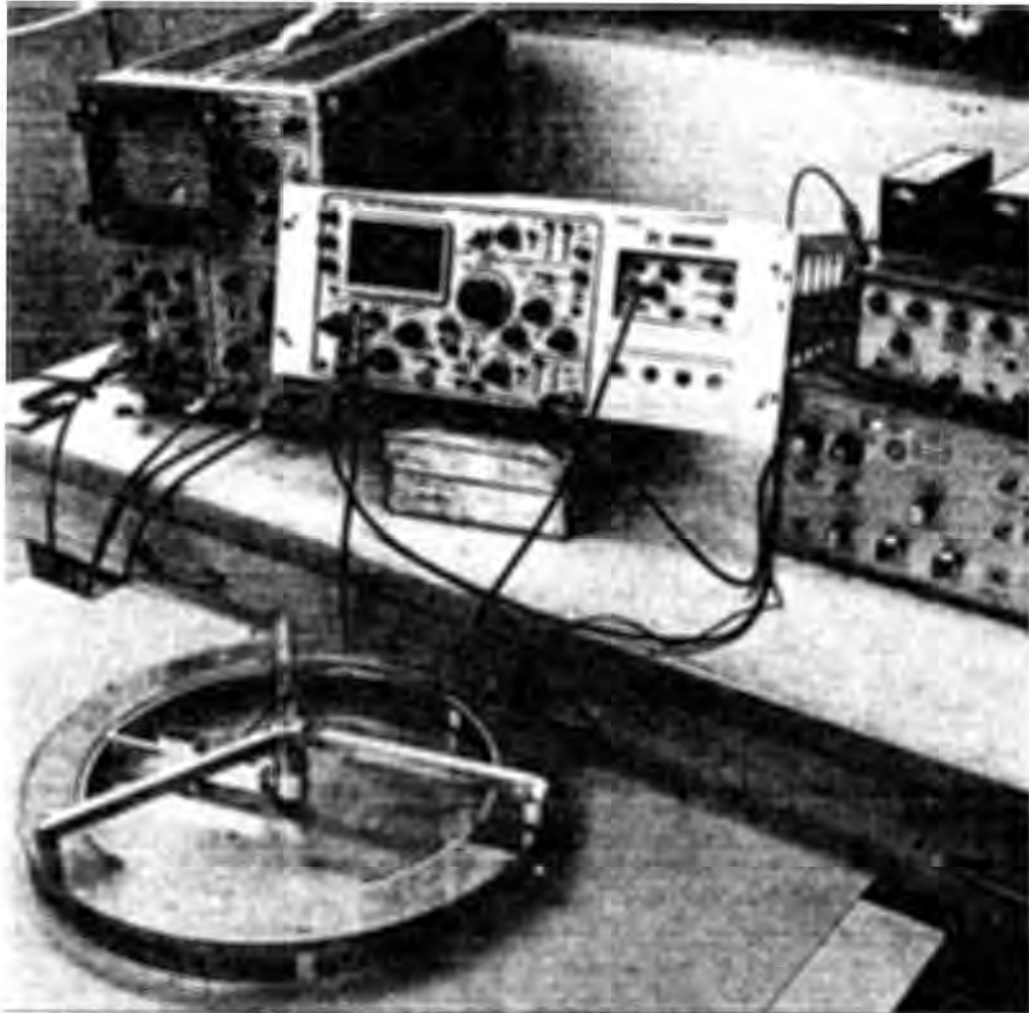


Fig. 3 Photo of apparatus, sample holder, and transducer goniometer.

by a surface distribution of equivalent body forces. This force distribution is then approximated and normal mode techniques are used to find the scattered amplitude. These theoretical approaches apply in the same regime as is of interest here and show agreement with the experimental results for angular scattering reported on here. However, in the frequency response the theory does not predict the resonances observed experimentally, although showing agreement with the background radiation.

We have formulated a model which we have found useful in analyzing both the angular and frequency dependencies of the Rayleigh wave scattering by a surface crack. This model is based on geometrical and optical diffraction theory and is applicable when the crack is long and deep compared to the Rayleigh wavelength. The interaction may be viewed as being concentrated near the surface, since the fields of the wave propagating on the free surface diminish rapidly or decay as they reach deeper into the material and are unable to probe the region near the crack tip. In this context the back-scattered radiation pattern is the Fourier transform of the complex amplitude distribution across an irradiated aperture. In general, using

the mathematical expression of the Huygens-Fresnel principle,²⁴ we can write the field amplitude at point (u_0, v_0) as

$$U(u,v) = \iint_{-\infty}^{\infty} h(u,v; x,y) U(x,y) dx dy \quad (5)$$

where $h(u,v; x,y) = (1/i\lambda) \frac{1}{r} \exp(ikr) \cos(\bar{n}, \bar{r})$ and

where $U(x,y)$ is the complex amplitude distribution across the aperture and is identically zero outside the aperture. k is the wave number and r is the distance between points (x,y) and (u,v) . $\cos(\bar{n}, \bar{r})$ is the obliquity factor and is approximately equal to one in this case where the distance to the detector is much greater than the maximum linear dimensions of the aperture and only a finite region about the aperture normal is used. The distance r is given by $r^2 = R^2 + (u-x)^2 + (v-y)^2$. If the Fraunhofer approximation $R \gg \frac{1}{2} k(x^2 + y^2)$ is adopted, the quadratic phase factor is approximately unity of the entire aperture and the observed field distribution can be found directly from a Fourier transform of the aperture distribution itself. Thus

$$U(u,v) = C \iint_{-\infty}^{\infty} U(x,y) \exp[-(ik/R)(ux+vy)] dx dy \quad (6)$$

where $C = (1/i\lambda R) \exp(ikR) \exp[(ik/2R)(x^2 + y^2)]$

For a rectangular aperture with apertures ℓ_x and ℓ_y normally illuminated by a unit-amplitude, monochromatic wave

$$U(u,v) = C \ell_x \ell_y \text{sinc}(\ell_x f_x) \text{sinc}(\ell_y f_y)$$

where $f_x = u/\lambda R$, $f_y = v/\lambda R$ are the frequencies at which the Fourier transform is evaluated. The intensity (square of absolute value of U) is

$$I(u,v) = \frac{\ell_x^2 \ell_y^2}{\lambda^2 R^2} \text{sinc}^2 \frac{\ell_x u}{\lambda R} \text{sinc}^2 \frac{\ell_y v}{\lambda R} \quad (7)$$

In the context in which the interaction between the surface waves and the crack is viewed, the result is specialized to a very narrow aperture of length $2a$, such that the intensity is approximately given by

$$I(\alpha, \theta, \omega) = I(0,0,\omega) (\sin^2 \psi) / \psi^2 \quad (8)$$

$$\psi = (a\omega/V_R)(\sin \alpha + \sin \theta)$$

where ψ takes into account oblique incidence of the radiation from the transmitter with an angle α to the aperture normal. In a backscattering experiment (typically encountered in a commercial application) $\alpha = \theta$ where θ is the angle of the receiver with respect to the crack normal. V_R is the Rayleigh wave velocity, ω is the frequency in radians and $I(0,0,\omega)$ is the intensity at $\alpha = 0$, $\theta = 0$ at a given frequency.

Angular Dependence

The results are summarized in Figs. 4, 5 and 6 where data and calculations are presented for the three types of experimental conditions. All three figures are similar in that they show structure typical of diffraction patterns, normalized at $\theta = 0$, i.e., the direction normal to the crack plane. The theoretical curves (solid line) are compared with the experimental data (dashed line) with a fit at $\theta = 0$. Considering the experimental errors in angle determination especially of the crack plane normal, reasonable agreement is observed between theory and experiment, especially in the positions of the nulls and peaks.

Considering the simplicity of the model the comparison with the experiment in the intensities is interesting. The experimental intensity curves generally fall above the theoretical curves, especially for the cracks in the ceramic samples. A tentative explanation is based on previous work on scattering from rough surfaces²⁵ which demonstrated that this behavior represents a diffuse back-scattering as from rough surfaces rather than the ideal scattering from a perfect planar reflector. This suggests the presence of

roughness inside the crack, that is the crack face is not smooth but rough, and it is obvious that the crack made by the indentation technique is much rougher than that made by spark erosion technique. A following step in the experiments is to use the results to interpret the degree of roughness of the crack face from the deviation of intensities from the ideal diffraction intensities. An additional source of deviation at large angles off broadside may perhaps be attributable to the inadequacies of the model. Auld et al⁷ have shown that for angles $\theta \gg 10$ in backscatter experiments the Born approximation begins to yield higher amplitudes for the higher order sidelobes.

Frequency Dependence

Equations (5) and (6) show that the frequency dependence of the radiation pattern at fixed angle may also be used to derive information on the crack radius. This is demonstrated in Fig. 7 which shows the frequency dependence of back-scattered power from the spectral analysis of a broad-band pulse for a semi-circular slot of radius $a = 800 \mu\text{m}$ indented into a plate of aluminum. As predicted, the graph shows the same type of diffraction pattern as those in the angular dependence studies. While this graph was obtained for $\theta = 18$, similar graphs may be generated quite readily for other angles. Such data may then be stored in the computer which can then be called upon to present the data with either angle or frequency as independent variable to show the complete equivalence of $\sin \theta$ or frequency as parameter. Figure 6 is actually a graph of the angular dependence as reconstructed at one frequency from a compilation of frequency dependence graphs obtained at various angles.

Inversion

The fields $U(x,y)$ and $V(u,v)$ in Eq. (6) are related by a two-dimensional Fourier transform. The inverse transform may be used to give the source distribution $U(x,y)$ from the measured or otherwise known remote field distribution,

$$U(x,y) = C \iint_{-\infty}^{\infty} U(u,v) \exp[-(ik/R)(ux + vy)] dx dy \quad (9)$$

Carrying out a procedure to evaluate (9) from known or measured field distributions constitutes the inverse scattering problem. The specific implementation of Eq. (9) is dependent of the nature of the field distribution and data format.

At this point the specific objectives of Section II come into play and the inversion is specialized to merely obtaining the fracture mechanics parameters, i.e., crack length and depth. Since the crack depth determination is accomplished by another procedure as discussed in section (5), the inversion procedure here need only provide a determination of the crack length. The Fraunhofer radiation pattern described in Eq.(8) is ideally suited to accomplish such a calculation by virtue of the nulls in the sinc function. The crack radius a is obtained by calculations based on the observed positions of the nulls in the angular

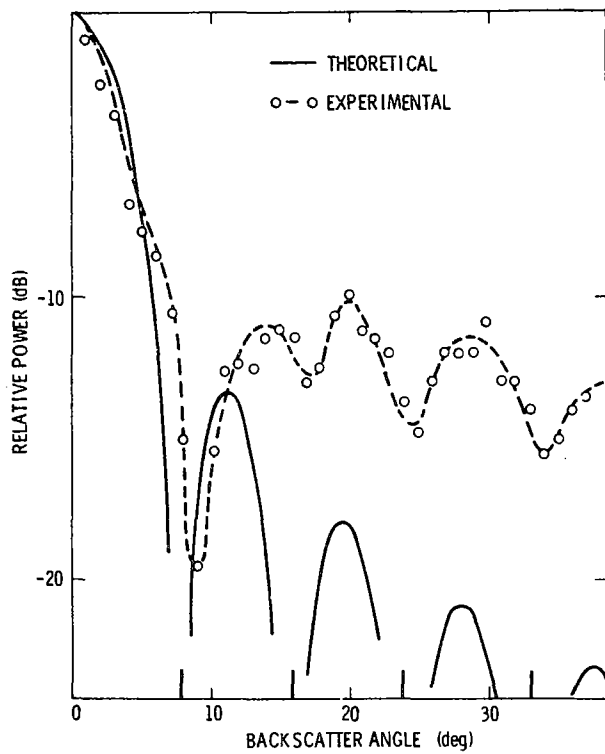


Fig. 4. Plot of relative power as a function of the back-scatter angle in acoustic surface wave experiments. The data, averaged over several runs, are for a sample of silicon nitride with a crack of radius $100 \mu\text{m}$ illuminated by wave of $\lambda = 55 \mu\text{m}$ in a narrow band experiment at 100 MHz. The crack was produced by the indentation technique.

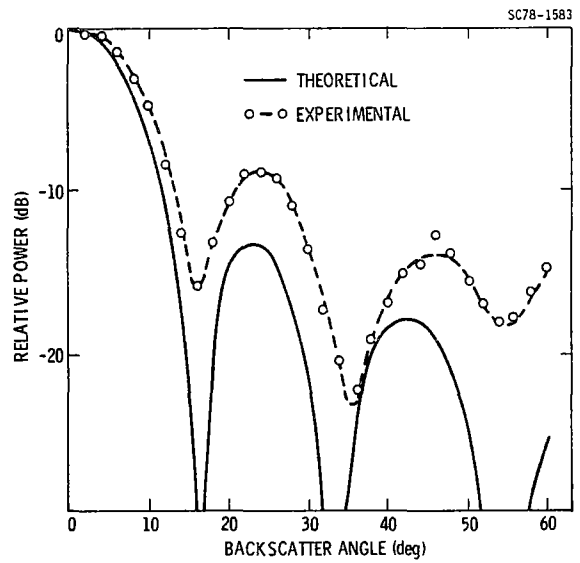


Fig. 5. Angular dependence of power of 2.2 MHz surface waves ($\lambda = 1293 \mu\text{m}$) back-scattered from a semi-circular slot of radius $1190 \mu\text{m}$ cut into commercial rolled aluminum by spark erosion technique.

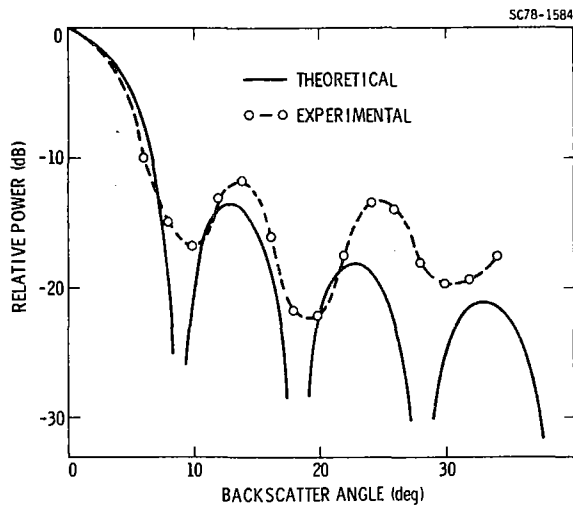


Fig. 6. Reconstruction of angular dependence of back-scattered power from spectral analysis of broadband pulses. The points were deduced at one frequency, i.e., 5 MHz ($\lambda = 585 \mu\text{m}$) from a series of spectra obtained for a variety of angles. The results are for a semicircular slot (radius $a = 900 \mu\text{m}$) indented into a plate of aluminum.

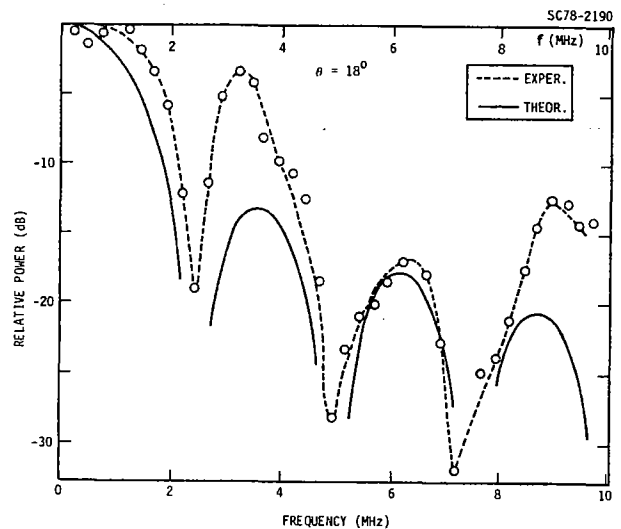


Fig. 7. Frequency dependence at fixed angle ($\theta = 18^\circ$) of back-scattered power from spectral analysis of broadband pulses for semicircular slot (radius $a = 900 \mu\text{m}$) indented into a plate of aluminum

(α, θ) or frequency (ω) dependence of the radiation pattern, for example: from the positions of the n^{th} null from broadside

$$a = \frac{n V_R}{\omega} / (\sin \alpha + \sin \theta). \quad (10)$$

Since each of the nulls, by virtue of its position, can be used to predict the length of the crack with the aid of the model, a statistical distribution of estimates may be obtained, and this is demonstrated in Table II. The comparisons between the crack (slot) radii estimates and the "actual" values obtained by micrographical examination show agreement within about 10 percent. The crack lengths estimated from the data are at most equal to real crack lengths because of the shape of the crack under the surface which provides a diminishing "effective" crack length with depth.

TABLE II
COMPARISON OF ESTIMATED AND "ACTUAL" CRACK RADIUS "a"

Experimental conditions	Diffraction order	Angular positions of nulls (deg)		Estimate of "a" (μm)	Mean estimate of "a" (μm)	"Actual" size of "a" (μm) [1 mil = 25.4 μm]
		Observed	Theoretical			
100 MHz silicon nitride with indentation crack	n = 1	9	8	87	93 \pm 4	100 \pm 3
	n = 2	17	16	92		
	n = 3	25	24	96		
	n = 4	34	33	97		
2.2 MHz commercial rolled aluminum with spark erosion slot	n = 1	16	16	1170	1160 \pm 20	1190 \pm 20
	n = 2	35	33	1130		
	n = 3	55	54	1180		
5.0 MHz Duraluminum with indentation slot	n = 1	10	9	866	880 \pm 16	900 \pm 25
	n = 2	19	18	897		
	n = 3	30	28	877		

* determined by micrographical examination of crack outline on sample surface.

Crack Depth Determination

For semi-circular cracks, the treatment given above is sufficient to provide a good estimate for the crack dimension. However, whenever elliptical-shaped cracks are encountered, the crack depth or, at least, the crack depth-to-length ratio must also be obtained for use in, for example, fracture mechanical life predictions.

The crack depth is readily derived from measurements of the same type as described above. Figure 8 shows a graph of the scattered amplitude as a function of the frequency for a slot of length 0.254 cm and depth 0.039 mm spark erosion cut into a plate of commercial aluminum. In contrast to the previous experiments which were pulse-echo, the results discussed here are for a fixed transmitter oriented normal to the slot face and a receiver whose angular position is allowed to vary. The principal feature of the graph is a peak at 3.45 MHz which remains stationary in frequency as the receiver angle is increased, in contrast to the other peaks which form a background that changes rapidly with angle (see for example the curve marked $\theta = 30^\circ$). The stationary peaks correspond to surface waves traveling along the slot face down to the slot tip and back up again to surface of the plate. The depth b is given by

$$b = V_R / 2f_b \quad (7)$$

The peak arises because of interference between the waves scattered from the crack tip and those scattered by the edge where the slot breaks the surface of the plate. The accuracy of the crack depth estimation by this technique is given in Table III for two different crack depths.

SC78-2191

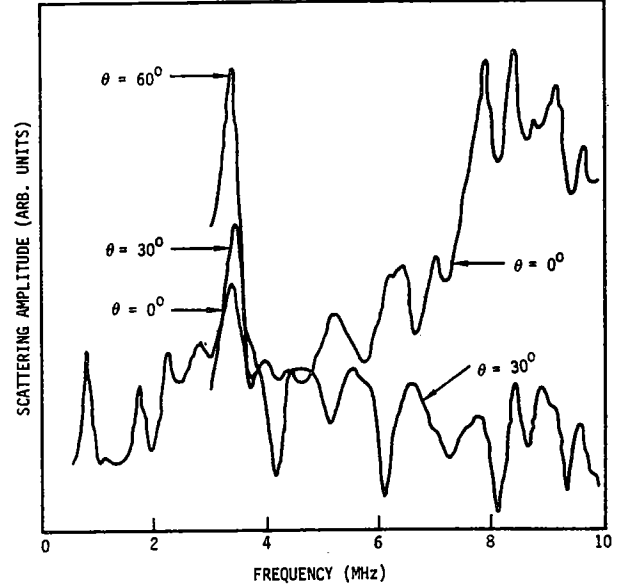


Fig. 8. Frequency dependence of scattering amplitude (pitch-catch) for an elliptically shaped slot (length 0.254 cm, depth 0.038 cm) in a plate of commercial aluminum.

TABLE III
CRACK DEPTH ESTIMATION

Transd Angle (deg)	Observ. Res (MHz)	Estim. Depth (mm)	Mean Estim. Depth (mm)	"True" Depth (mm)	Percent Error (%)
0	3.45	.412	0.408	0.38	3%
30	3.47	.409			
60	3.40	.418			
90	3.40	.418			
120	3.42	.415			
150	3.50	.406			
180	3.45	.412			
210	3.50	.406			
240	3.90	.364			
270	3.40	.418			
0	1.34	.107	0.104	0.102	2%
20	1.34	.107			
30	1.33	.106			
45	1.32	.099			
60	1.60	.089			
75	1.35	.105			
90	1.22	.116			

Domarkas et al⁶ have recently reported observing peaks in the frequency dependence of the Rayleigh wave reflection coefficient obtained normal to rectangular slots. They have interpreted these peaks in terms of resonances within the slot, i.e., when the depth of the crack is a multiple of a half-wavelength long the top surface displacement tends to be very small, as it is at its tip and so there is again a maximum in the reflection coefficient of a wave incident on the crack. One may infer from this interpretation that the resonances are essentially standing surface waves with quasi-nodal points at the tip of the crack and the top surface. It appears to us that this interpretation has difficulties, since these points are stress-free boundaries and should not in general correspond to points of minimum displacement.

Short Pulse Studies

Another manifestation of the diffraction discussed above lies in time domain studies. These are particularly effective for oblique interrogation of the crack. The situation is illustrated in Fig. 4 for a surface wave incident normal to the crack plane and a receiver scattered at a large angle from the normal. In the case of very short pulses the diffraction pattern can be interpreted as coming from two point sources located at the crack tips. For sufficiently short pulses, the pulses from the two sources can be resolved in the time domain and lead to interference in the frequency domain. Figure 5 shows experimental data obtained with a slot of length $a = 0.254$ cm and the receiver oriented along a direction in the plane of the slot. The separation of the pulses is in good agreement with a time-delay calculated on the basis of a Rayleigh wave traveling along the length of the slot. Good agreement is also observed between the observed and calculated pulse separation at angles other than 90° as is indicated in Table IV.

TABLE IV
TIME DOMAIN PULSE SEPARATION
FOR 0.254 cm x 0.254 cm SLOT

Receiver Angle θ (degs)	Observed $\Delta\tau$ (μsec)	Theor. $\Delta\tau$ (μsec)
0	0	0
30	.4	.45
60	.7	.77
90	.9	.89

The existence of two somewhat separated pulses in the time domain is equivalent to interference in the frequency domain and Fig. 10 shows the magnitude of the Fourier Transform of the time

domain signal of Fig. 9. Also shown are the calculations corresponding to the model described earlier in good agreement with the experiment with respect to the positions of the nulls and peaks. This comparison is shown more quantitatively on Fig. 11 which plots the null frequencies f_m versus the null indices m for several receiver angles. The straight lines labeled "theory" are derived on the basis of

$$f_m = m V_R / 2a \sin \theta.$$

where as before $2a$ is the slot length and V_R is Rayleigh wave velocity.

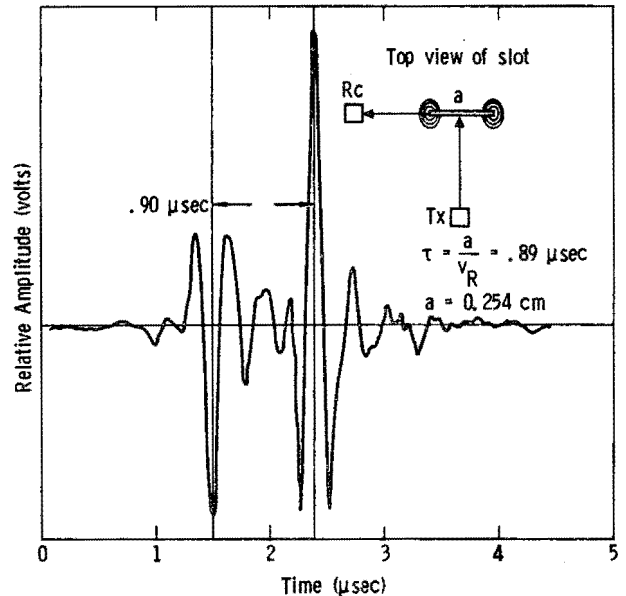


Fig. 9. Time-domain r.f. wave form of signal scattered from slot (length 0.254 cm) irradiated at normal incidence.

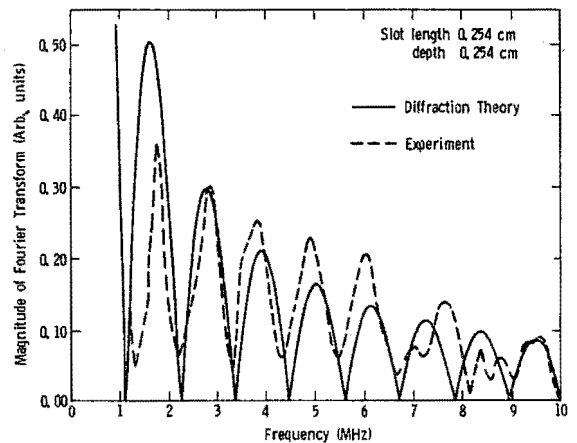


Fig. 10. Waveform of Fig. 9 in frequency domain.

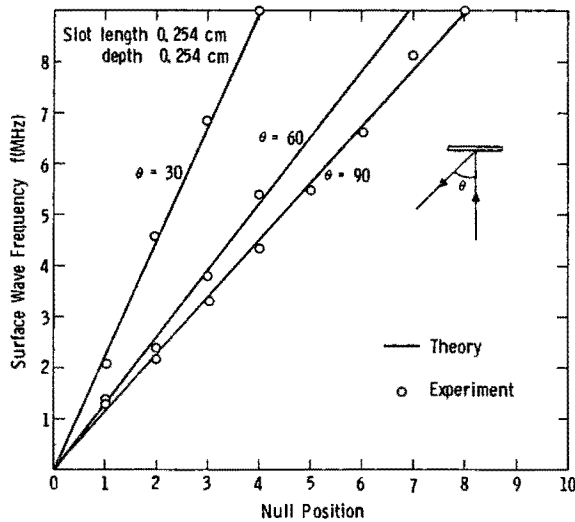


Fig. 11. Frequency domain location of nulls as a function null index for data such as shown in Fig. 10.

Fracture Mechanical Predictions

With the techniques described above we have examined six slot/crack configurations with various depths and lengths and have calculated the reduced stress intensity factors $K_I = K_I / \sigma_{max}$ (which describes, basically the geometry of the crack--see Eq. (1)) and qualitatively predicted the direction of crack growth based on an assumed applied stress parallel to the specimen surface and the slot/crack plane. This information is summarized in Table V. For example, the crack in silicon nitride having a length of 0.4 mm and a depth of 0.2 mm has a $K_I = 0.40 \sqrt{\text{mm}}$ and is going to grow in the direction $\psi = 0, \psi = 180$ or in a direction along its length (see Fig. 2a). On the other hand, the spark eroded slot (in commercial aluminum) with dimensions 2.5 mm in length and 0.4 mm in depth has a $K_I = 1.11 \sqrt{\text{mm}}$ and will grow deeper in a direction normal to the surface.

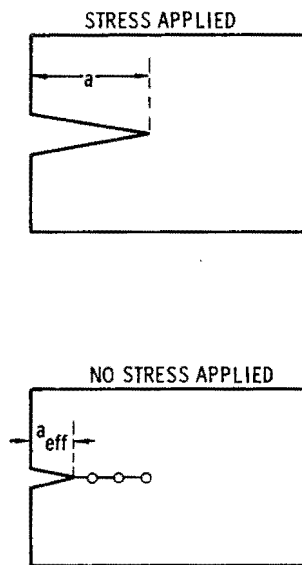
TABLE V

FLAW SIZE	TYPE/MATERIAL	$k_I (\sqrt{\text{mm}})$	CRACK PROP
	EDM/ALUMINUM	1.11	$\psi = 90^\circ$
	EDM/ALUMINUM	1.26	$\psi = 90^\circ$
	EDM/ALUMINUM	1.41	$\psi = 0^\circ, 180^\circ$
	CRACK/SI-NITRIDE	0.40	$\psi = 0^\circ \dots 180^\circ$
	EDM/ALUMINUM	1.41	$\psi = 0^\circ \dots 180^\circ$
	CRACK/ALUMINUM	1.21	$\psi = 0^\circ \dots 180^\circ$

Crack Closure

Part-through crack growth in ductile materials is often associated with partial crack closure as the applied stress is changed dynamically such as during fatigue cycling or as a function of time during stress relaxation. The process is shown in more detail in Fig. 12 which displays schematically a crack in the absence and presence of applied stress. On unloading, a crack starts to close down on itself at a stress level σ_{cc} , the so called closure load. Unloading the specimen completely leaves the crack partially open, however, due to excessive compressive stresses along the closed fracture stress area. An NDE measurement capable of determining effective crack depth during partial crack closure would be important since it could determine quantities such as the crack closure stress, residual stress, and time dependent stress relaxation which are important parameters that modify Eqs. (1) and (2).¹³

PART-THROUGH CRACK GROWTH IN DUCTILE MATERIALS



CRACK CLOSES DOWN AT CRACK CLOSURE STRESS σ_{cc}

$$\text{SO THAT } \Delta\sigma = (\sigma_{\max} - \sigma_{cc})$$

Fig. 12. Schematic of part-through crack in presence and absence of applied stress.

The crack depth measurements described above with the use of surface waves appears to represent a promising technique to shed light on this question. The position of the crack depth in the frequency domain would be observed as a function of the applied stress and interpreted in terms of the degree of partial crack closure. Under ideal conditions the peak amplitude might give information on the nature of the crack tip and distinguish between temporary mechanical crack closure and crack healing. Experiments along these lines are now in the planning stage and will be reported on in the near future.

CONCLUSION

This report presents results on a simple approach to describe the size of surface breaking flaws. The scattered radiation patterns of the flaws when irradiated by acoustic surface waves are interpreted to provide estimates of flaw length and depth with an accuracy of 10% or better. The key features are the positions and spacings of nulls or

peaks in the angular and frequency dependence of scattered energy in either pitch-catch or pulse echo. A simple model based on optical diffraction theory is presented and demonstrated. The good agreement between this model and the experimental observations is interesting since it provides - at least to first order - an analogy between the behavior of the surface waves and that of electromagnetic waves. While the results presented here are useful for estimation of the size of simply shaped, surface breaking flaws, much more work must be carried out to extend the technique to include all possible situations encountered in fracture mechanics. Such circumstances as cracks inclined to surface, crack with severe surface roughness, nonelliptically-shaped cracks, roughness of the specimen surface, crack closure of fatigue cracks, to name a few, must be taken into account.

ACKNOWLEDGEMENT

The authors are indebted to P. Khuri-Yakub for the design, construction, and demonstration of the 100 MHz surface wave transducers (see Ref. 2) used in one of the three experiments, to A. E. Evans for the preparation and characterization of the half-penny shaped crack in the ceramic sample. The authors are also grateful to H. Nadler for the design of 100 MHz goniometer, to J. Doucet for the construction of the low frequency goniometers, and to C. Picard for the micrographical examination of the samples. The first part of this work was carried out in France at the "Groupe de Physique des Solides de l'Ecole Normal Supérieure," during B. R. Tittmann's stay as "Professor Associe" at the University of Paris VIII, and was supported by the CNRS (Centre National de la Recherche Scientifique). This work was later complemented by work done at the Science Center and one of the author's (B.R.T.) research was sponsored by the Center for Advanced NDE operated by the Science Center, Rockwell International, for the Advanced Research Projects Agency and the Air Force Materials Laboratory under Contract F33615-74-C-5180.

REFERENCES

1. P.A. Doyle and C.M. Scala, *Ultrasonics* **16**, 164 (1978).
2. B.T. Khuri-Yakub and G.S. Kino, *Appl. Phys. Lett.*, **32**, 513 (1978).
3. J.D. Fraser, B.T. Khuri-Yakub, and G.S. Kino, *App. Phys. Lett.*, **32**, 698 (1978).
4. M.T. Resh, B.T. Khuri-Yakub, G.S. Kino and J.C. Shyne, *Proceedings of the First International Symposium of Ultrasonic Material Characterization at Gathersburg, Md., June 1978* (in press).
5. G.S. Kino, *J. Appl. Phys.* **49**, 3190 (1978).
6. V. Domarkas, B.T. Khuri Yakub, G.S. Kino, *Appl. Phys. Lett.* **33**, 557 (1978).
7. B.A. Auld, S. Ayter and M. Tan, 1978 *Ultrasonics Symposium Proceedings*, IEEE Cat. No. 78, Ch. 1344-1SU, in press.

8. B.R. Tittmann, F. Cohen-Tenoudji, M. De Billy, A. Jungman and G. Quentin, *App. Lett.* 33, 6 (1978), see also 1978 Ultrasonic Symposium Proceedings IEEE, Cat. No. 78, Ch. 1344-1SU, in press.
9. J.E. Collipriest, Jr., *The Surface Crack* (edited by J.L. Swedlow) *The Am. Soc. of Mech. Eng.*, 43 (1972).
10. G.R. Irwin, *J. Appl. Mechanics* 29, 651 (1962).
11. P.C. Paris and F. Erdogan, *J. Basic Eng.* 85, 528 (1963).
12. H.W. Reinhardt and J.W. Dally, *Mat. Eval.* 30, 213 (1970).
13. O. Buck, J.D. Frandsen, and H.L. Marcus in *Fatigue Crack Growth Under Spectrum Loads*, ASTM STP 595, *Am. Soc. Testing and Materials* 101 (1976).
14. M.G. Silk, *NDT Int.* 9, 290 (1976).
15. D. Cook, *Proc. Brit. Acoust. Soc. Spring Meeting, Loughborough*, 72 U19 (1972).
16. R.L. Hudgell, L.L. Morgan, and R.F. Lumb, *Brit. J. Nondestructive Testing* 16, 144 (1974).
17. K.G. Hall, *Nondestructive Testing* 9, 121 (1976).
18. B.H. Lidington and M.G. Silk, *Brit. J. Nondestructive Testing* 17, 165 (1975).
19. O.R. Gericke, *Ultrasonic Spectroscopy*, Ch. 2 in *Research Techniques in Non-destructive Testing*, Ed. R.S. Sharpe, Academic Press, London and N.Y. (1970).
20. A. Brown, *Ultrasonics* 11, 202 (1973).
21. L.L. Morgan, *Acoustica* 30, 222 (1974).
22. J.J. Petrovic and M.G. Mendiratta, *Jnl. Amer. Ceram. Soc.*, 59, 163 (1976).
23. Y.D. Achenbach, private communication.
24. Y. Goodman, *Fourier Optics*, McGraw-Hill Book Company New York, 1968.
25. M. DeBilly, F. Cohen-Tenoudji, A. Jungman and G. Quentin, *IEEE Trans. on Sonics and Ultrasonics S.U.* 23, 356-363 (1976).

DISCUSSION

Gordon Kino (Stanford University): Bernie, have you experienced any difficulties in observing tight cracks? We had some experience with glass, for instance. We had to take the precaution of putting a little bit of stress on it to make sure the crack was open to get the full area of the crack.

Bernie Tittmann (Rockwell International Science Center): Yes, if you noticed in one of the tables where I list the predicted crack radii and compare them to the true crack radii, you find that the experiments underestimate the answers. We associate that partly with the tightness at the crack edges, but also the fact that, after all, the surface waves impinging on an elliptically shaped crack sample, not just the top part, but also the flanks of the crack which are, in fact, narrower. I think we will address that problem with our fatigue specimens where, of course, we can control the crack opening at will.

Gordon Kino: Actually watch it change?

Bernie Tittmann: Yes.

Gordon Kino: That will be nice.

R. E. Green (Johns Hopkins): Are you going to measure the crack opening continuously with ultrasound while you are fatiguing it?

Bernie Tittmann: Yes.

SUMMARY COMMENTS

John Brinkman, Chairman (Rockwell International Science Center): There is one item scheduled yet on the program you will notice called Summary Comments. We would ask you, we will promise you, this won't be very long, but we do have two more people that would like to speak. I will tell you, first of all, that the second of these is Don Thompson. Don's remarks will be short.

The first one is Gary Laurentzen. Gary is with the Naval Ship R & D Center and is going to tell us briefly, about the tour to the Naval Development and Training Center, Fleet Maintenance Assistance Group-Pacific.

Cary Laurentzen: The Command that I am with is staffed by about 1700 to 2000 sailors, mostly of the senior rates. Although we don't pursue research, our purpose is to try to develop them as better sailors and provide them some training ashore.

With regard to your own interests, on the tour this afternoon we will back up a little bit and return you to earth, so to speak. In terms of what we have, we are using several nondestructive testing techniques. This was, I guess, a step from nothing in terms of what the Navy was using. We are beginning, however, to use a greater number of procedures. We have been a Command for about ten years or so. It was designed originally in Admiral Zumwalt's day to try to give the sailors a billet ashore because they are at sea all the time. Then we decided to train them in ship repair techniques. The Command is really someplace in between a floating repair ship and a shipyard because we don't have the real experienced personnel that a shipyard would have, but we do an awful lot of similar work.

We have a number of facilities at the Command. These include testing facilities as well as chemical and metallurgical laboratories. These facilities are central to other activities at the Command. For example, we do a considerable amount of pipeshop work. One of the areas where we use nondestructive testing is to determine what piping needs to be renewed. We use ultrasonic techniques to try to measure piping thickness sometimes before it is removed from the ship.

Another area is welding. I would say 50 to 60 percent of our nondestructive testing involves the inspection of welds. A lot of it is done in the shop, an immense amount of welding is also done aboard ship.

A third area of interest is the lagging shop. There has been much publicity recently on asbestos. We are trying to develop a means to identify the presence of asbestos in lagging. In the older ships, the lagging may contain asbestos which is used to insulate steam piping. If you have any ideas concerning identification of asbestos, I would surely like to have that. We also use NDT procedures in our foundry. We pour some of the more exotic alloys. We do have to radiograph some castings, and we will do some ultrasonics on them. We do not have any shear wave capabilities. This is sort of the next step for the Navy. An additional use for NDT procedures is in oil analysis to detect engine wear. The Navy has quite a campaign now in attempting to use this technique for the diesel engines in which we perform spectroscopic examinations of oils after every hundred hours or so to detect the presence of wear metals and determine how soon we may need to overhaul an engine.

The corrosion and erosion of pumps in salt water environments is a major problem area in terms of ship maintenance. We are not doing too much in terms of NDE in this area. It is just a matter of finding an alloy that will hold up under this type of environment where we have so many problems.

This has been a short preview of what you will see on the tour. I hope it will be of interest to you. As I said, we are not a research Command, but we would certainly appreciate any comments from you as you observe our work that would improve our NDE activities. Thank you.

John Brinkman, Chairman: Thank you Gary. Before I can Don up here, I just want to say I know I speak for everyone here and everyone who has been here this week in wanting to express our gratitude to Don for everything that he has done to make this conference possible. I learned he does some things that I didn't know he did. As a matter of fact, I found myself with him on a couple of occasions and ended up doing carpentry work, janitorial work and a few other things. Really, Don personally looks after everything from a long time before this conference takes place until a long time afterward. I think that we should give Don a hand before asking him to come up here for his final remarks.

Don Thompson (Rockwell International Science Center): Thank you for the very kind remarks, John. I just have a few comments to make in the way of acknowledgments before we close. I wish to thank you all for coming to the meeting. I wish also to acknowledge the people at Scripps. We have had good cooperation from the people at the Scripps organization. We also had a number of overseas visitors whom we want to welcome. I would also like to acknowledge the many good works interactions that participants of this program have had with the ARPA Materials Research Council. Some of the MRC work, in parallel with work in this program, has really been of importance in bringing about key advances in this area. In this context I especially want to acknowledge the contributions of MRC members W. Kohn, B. Budianski, J. Rice and R. Thomson. I would also like to thank Mrs. Diane Harris and Mrs. Nadine Brinkman for their excellent work in arranging and managing the many details associated with this meeting. If you feel inclined I think they are still outside the door and as you go out

you might like to give them a thanks.

Finally, I would like to thank both ARPA and AFML for their support in this work and for the privilege of being able to present it at a meeting like this. The proceedings of the meeting will be published as an Air Force Materials Lab report. Those of you who are registered at this meeting should receive a copy in the mail.

Many thanks to Mr. Jim Kelly and Mr. Gary Laurentzen of the Navy in preparing the tour this afternoon. I think it will be an interesting tour and I hope you will be able to participate in it. It is always a revelation, I think, for a research person to see the environment in which his product eventually must be used. It is enough to make one throw up his hands in despair at times, but it is a worthwhile experience in the sense that it often suggests different approaches to research if you know something of the final geometric and environmental constraints in which it has to be used.

With that, I think I have nothing more to say. I will repeat the announcements that Mike made this morning. The desire is to hold the meeting here at Scripps again next year. I certainly endorse that. The grounds, the surroundings, the climate, the people, have certainly all been cooperative. Again, thank you.